

Structural and mechanical properties of CuZr/AlN nanocomposites

Man GU^{1,2}, Yu-cheng WU^{1,3}, Ming-hua JIAO^{3,4}, Xin-min HUANG¹

1. School of Materials and Engineering, Hefei University of Technology, Hefei 230009, China;
2. Department of Mechanical Engineering, Hefei University, Hefei 230022, China;
3. Engineering Research Center of Powder Metallurgy of Anhui Province, Hefei 230009, China;
4. Institute of Tribology, Hefei University of Technology, Hefei 230009, China

Received 11 January 2013; accepted 25 October 2013

Abstract: Powder metallurgy method was used to prepare copper alloy nanocomposites (CuZr/AlN) with high strength and conductivity. Optical microscopy, high-resolution transmission electron microscopy and other methods were adopted to study the impact of different sintering technologies on the structural and mechanical properties as well as the impact of solution and aging treatments on the mechanical properties of CuZr/AlN. The result shows that the specimen has a dense structure, and the size of the crystal grain is around 0.2 μm . The Brinell hardness of the specimen increases with the increase in re-pressing pressure and sintering temperature. The Brinell hardness of specimen also increases with the increase in zirconium content. However, above 0.5% (mass fraction) of zirconium content, the Brinell hardness of the nanocomposites is reduced. The buckling strength of the specimens increases with the increase in re-pressing pressure and sintering temperature. The buckling strength is the highest when the zirconium content is 0.5%. The Brinell hardness is lower after solution and aging treatments at 900 °C. The Brinell hardness of the CuZr/AlN series specimen after the aging treatment at 500 °C or 600 °C increases. The specimen was also over aged at 700 °C.

Key words: CuZr/AlN nanocomposites; powder metallurgy; mechanical properties

1 Introduction

The component, structure, and property of materials are closely related. For the Cu–Zr series alloy, copper and zirconium can form numerous intergranular compounds. These copper alloys are widely applied due to their high strength and conductivity [1–3]. These alloys are mainly characterized by high electric conductivity [4,5]. ARNBERG et al [6] prepared a copper zirconium alloy, and Cu–0.15Zr alloys have excellent comprehensive properties by a high-pressure helium ultrasonic atomization method. The yield strength values of the alloys are as high as 406 MPa. The tensile strength values are as high as 460 MPa, and the electric conductivities are up to 91% (International Annealed Copper Standard). The Cu–Cr–Zr alloy is a copper alloy and has wide applications due to its high strength and electric conductivity. The chromium bronze has high

mechanical, thermal, and electric conductivity properties. With a higher crystallization temperature and better heat resistance, the alloy is stable below 400 °C. To improve the strength of the alloy, deformation treatment and RS treatment are often adopted [7,8]. Cu–Cr–Zr has a better comprehensive property than Cu–Cr or Cu–Zr alloy which are widely used at present [9,10]. However, many of the Cr and Cu₃Zr particles are precipitated by aging and dispersing [11]. Many reports discussed the impact of the microstructural changes of alloy after quenching, deformation treatment, thermochemical treatment, solution and aging treatments on the mechanical properties and revealed its application potential [12–16].

The current work adopted the powder metallurgy method and combined this with the re-pressing and re-sintering process to prepare high-strength and high-conductivity copper alloy nanocomposites (CuZr/AlN). Optical microscopy (OM) and high-resolution transmission electron microscopy (HRTEM) were used

Foundation item: Project (KJ2013A227) supported by the Natural Science Research Key Projects of Anhui Provincial Universities, China; Project (51104051) supported by the National Natural Science Foundation of China; Project (11C26213401903) supported by Innovation Fund for Small and Medium Technology Based Firms, China

Corresponding author: Yu-cheng WU; Tel/Fax: +86-551-62901012; E-mail: ycwu@hfut.edu.cn
DOI: 10.1016/S1003-6326(14)63072-7

to investigate the impact of different sintering processes on the structural and mechanical properties of the nanocomposites as well as the impact of solution and aging treatments on the mechanical property of the nanocomposites.

2 Experimental

Cu powder (grain size 47 μm , purity 99%) and Zr powder (grain size 40 μm , purity 99%) were mixed with AlN nanopowder (~ 50 nm) in composition (mass fraction, %) of Cu-0.3Zr-0.1AlN, Cu-0.5Zr-0.1AlN, Cu-1Zr-0.1AlN, Cu-3Zr-0.1AlN, and Cu-5Zr-0.1AlN. The products were named CZA1, CZA2, CZA3, CZA4, and CZA5. The samples were ball milled with a GN-2 type high-energy ball mill. A GCr15 bearing steel ball was used for ball milling after thermal refining. The mass ratio of the grinding media to the material was 10:1. Argon was used as protection during ball milling. The powder obtained after ball milling for 10 h was used in the experiment. The 769YP-40C performing machine was used for pressing. Products were sintered in a SK2-4-12 tube-type sintering furnace and protected with H_2 gas. The H_2 flow rate was controlled at 25 to 30 mL/s during sintering. Before heating, H_2 was fed into the furnace for 10 min. Heat flow was increased at a rate of 10 $^\circ\text{C}/\text{min}$. Re-pressing and re-sintering temperatures were 800 $^\circ\text{C}$ and 900 $^\circ\text{C}$, respectively, and sintering time was 90 min. Solution and aging treatments were conducted in vacuum at 900 $^\circ\text{C}$ for 1 h. Then, the materials were quenched at room temperature under high-purity and high-speed N_2 flow. After the solution treatment, the specimens were aged at 500, 600, and 700 $^\circ\text{C}$ for 1 h. The HB-3000C electric Brinell hardness tester was used to measure the hardness of the specimens. The hardness was the average of three points in the experiment. The MTS 809 axial/torsional test system was adopted for the bending-resistance test. An optical microscope and a JEM-2010 type high-resolution transmission electron microscope were used to observe the microstructure of the nanocomposites.

3 Results and discussion

3.1 Microstructure

Figure 1 shows the OM image of the CZA2 specimen after re-sintering at 800 $^\circ\text{C}$. An obvious contrast grade was caused by the uneven plane during the sample milling. Figure 2 shows the TEM image of the specimen after re-sintering at 800 $^\circ\text{C}$. Based on Figs. 1 and 2, the specimen has a dense structure, and the grain size is around 0.2 μm .

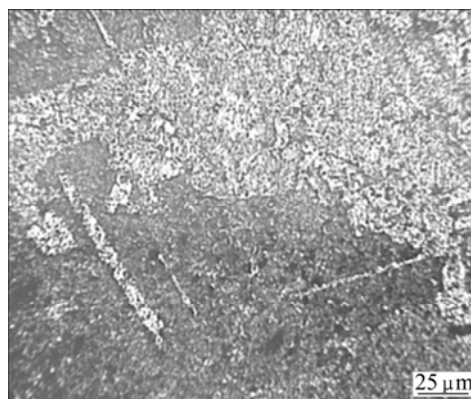


Fig. 1 OM image of CZA2 after re-sintering at 800 $^\circ\text{C}$

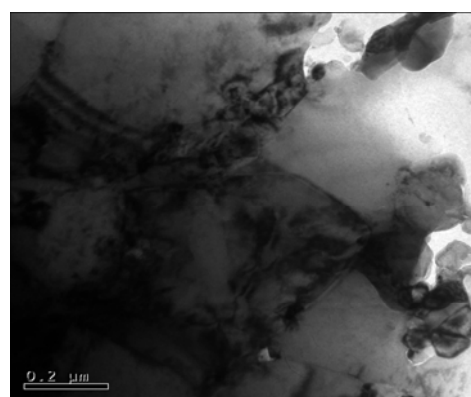


Fig. 2 TEM image of CZA2 after re-sintering at 800 $^\circ\text{C}$

3.2 Mechanical properties

3.2.1 Hardness analysis

Using the same component and re-sintering temperature, the Brinell hardness of composites increased with the increase in re-pressing pressure. Using the same component and re-pressing pressure, the Brinell hardness increased with the increase in sintering temperature from 800 $^\circ\text{C}$ to 900 $^\circ\text{C}$. The increase in re-pressing pressure or sintering temperature improved the density of materials. After sintering at 900 $^\circ\text{C}$, the grains became large and the Brinell hardness was reduced. However, the increase in density is the major factor that influences the Brinell hardness. Thus, if sintering temperature is increased, the Brinell hardness will be also increased. Figure 3 shows that the Brinell hardness of the nanocomposites increased with the increase in zirconium content. However, when the content of the zirconium was more than 0.5%, the Brinell hardness of the nanocomposites decreased. This phenomenon is explained by the particle strengthening theory. The nanophase and matrix phase blocked the dislocation because of the difference in material properties and spatial distribution. Considering the higher strength of the strengthening phase, the dislocation could not occur easily. Moreover, the spatial

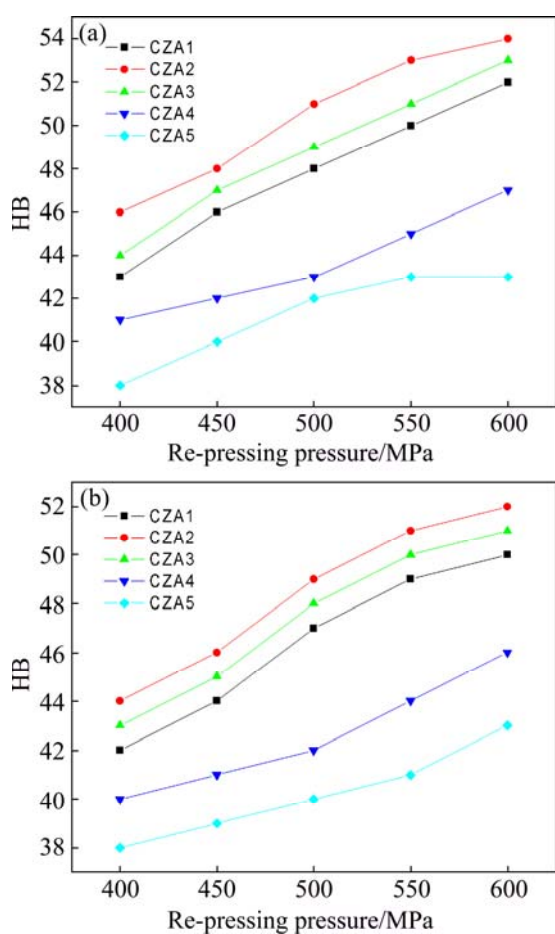


Fig. 3 Relationship between re-pressing pressure and Brinell hardness of CZA composite: (a) Re-sintering at 800 °C; (b) Re-sintering at 900 °C

distribution of the strengthening phase changed, impelling the direction of the dislocation. The co-actions of the two factors improved the overall resistance of the materials to deformation. Given the difference of material properties, differences should exist in all phases during plastic working. To maintain the continuity of the materials, a certain line defect should be increased to achieve a certain plastic deformation amount. The interaction of a large amount of line defect blocks the sliding deformation of materials and improves the flow stress of materials. Therefore, the strength of materials is increased, which is reflected by the increase in Brinell hardness. However, when the content of the nanoparticles is more than 0.5%, oxygen appears at the grain boundary because of the oxidation of zirconium. Thus, cuprous oxide is generated. This factor has great influence and reduces the Brinell hardness.

3.2.2 Bending strength

Figure 4 shows the relation curve of the re-pressing pressure and bending strength of the CZA composites. For the specimens with the same component, the bending strength increased with the increase in re-pressing

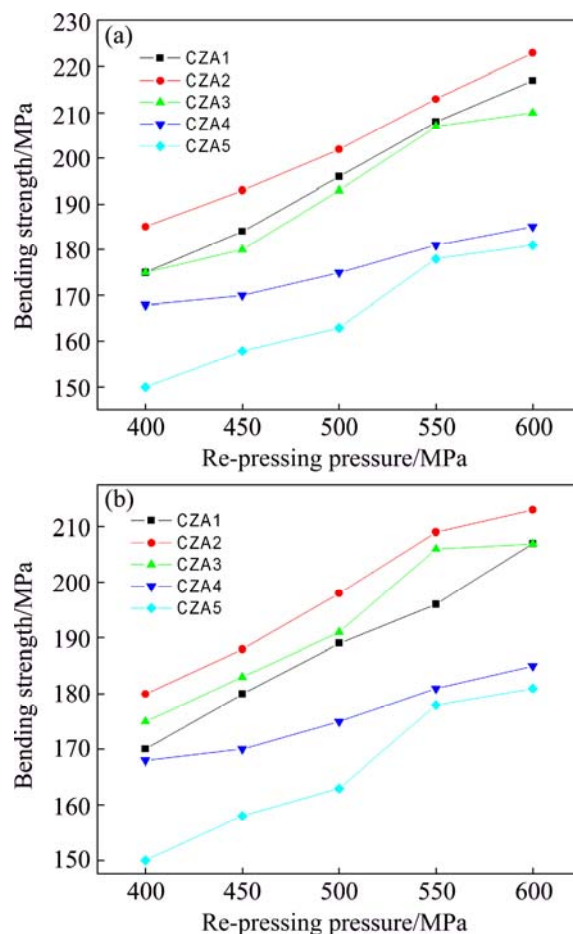


Fig. 4 Relationship between re-pressing pressure and bending strength of CZA composites: (a) Re-sintering at 800 °C; (b) Re-sintering at 900 °C

pressure. The bending strength also increased with the increase in sintering temperature. Using the same re-pressing and re-sintering process, the bending strength was the highest at 0.5% zirconium. Further increase in zirconium content resulted in a reduced bending strength. When the zirconium content increased, the oxidation of zirconium induced oxygen to generate cuprous oxide at the grain boundary, destroying the bending strength of the composites. The re-pressing and re-sintering process increased the bending strength of the specimen. Based on an existing empirical formula, bending strength is half the ultimate tensile strength. Thus, the maximum ultimate tensile strength of the CZA composites was around 440 MPa.

3.2.3 Impact of solution and aging treatments on mechanical property of CZA specimens

Figure 5 shows the relation curve of the solution and aging treatments and hardness of the CZA specimens that were re-sintered at 900 °C. The Brinell hardness after solution treatment at 900 °C was lower than that before the solution treatment, which indicates that the zirconium atoms were melted in the lattice of copper to

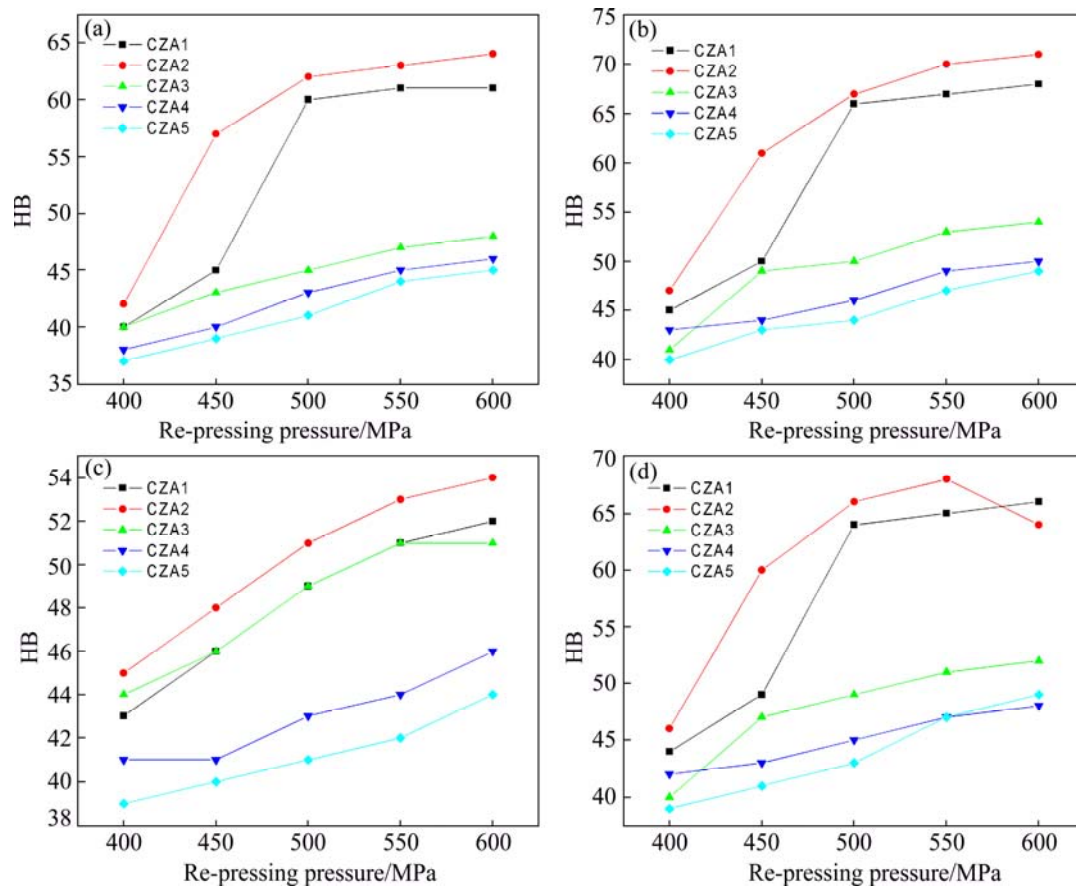


Fig. 5 Relationship between solution and aging treatments and hardness of CZA composites re-sintered at 900 °C: (a) After solution treatment at 900 °C; (b) After aging treatment at 500 °C; (c) After aging treatment at 600 °C; (d) After aging treatment at 700 °C

generate a copper–zirconium solid solution with face-centered cubic lattice structure. Thus, the Brinell hardness was reduced. As seen in Figs. 5(b) and (c), the Brinell hardness of the CZA specimens increased after the aging treatment at 500 °C or 600 °C. As seen in Fig. 5(d), the Brinell hardness of the specimens after the aging treatment at 700 °C was reduced, which shows that overaging occurred at this temperature.

4 Conclusions

1) CuZr/AlN nanocomposites were prepared by powder metallurgy. The structure of CuZr/AlN nanocomposites is dense, and the size of the crystal grain is around 0.2 μm.

2) The Brinell hardness of CuZr/AlN nanocomposites increased with the increase in re-pressing pressure, sintering temperature or zirconium content.

3) The bending strength of the specimens increased with the increase in re-pressing pressure or sintering temperatures. The bending strength was the highest when the zirconium content was 0.5%.

References

- JORDINA F, MARIA D B, SANTIAGO S. The influence of deformation-induced martensitic transformations on the mechanical properties of nanocomposite Cu–Zr–(Al) systems [J]. *Advanced Engineering Materials*, 2011, 13(1–2): 57–63.
- JITTRAPORN W N, MEGUMI K, TERENCE G L. Achieving homogeneity in a Cu–Zr alloy processed by high-pressure torsion [J]. *Journal of Materials Science*, 2012, 47: 7782–7788.
- AZIMI M, AKBARI G H. Development of nano-structure Cu–Zr alloys by the mechanical alloying process [J]. *Journal of Alloys and Compounds*, 2011, 509: 27–32.
- DENG Jing-guan, WU Yu-cheng, YU Fu-wen, WANG De-guang. Microstructure and properties of powder metallurgy Cu–Zr alloys [J]. *Rare Metal Materials and Engineering*, 2009, 38(z1): 205–208. (in Chinese)
- KIMURA H, INOUE A, MURAMATSU N, SHIN K, YAMAMOTO T. Ultrahigh strength and high electrical conductivity characteristics of Cu–Zr alloy wires with nanoscale duplex fibrous structure [J]. *Materials Transactions*, 2006, 47(6): 1595–1598.
- ARNBERG L, BACKMARK U, BÄCKSTRÖM N, LANGE J. A new high strength, high conductivity Cu–0.5wt.%Zr alloy produced by rapid solidification technology [J]. *Materials Science and Engineering*, 1986, 83: 115–121.
- SUN S, SAKAI S, SUZUKI H G. Effect of alloying elements on the cold deformation behavior of Cr phase and the tensile strength of

- Cu–15Cr based in situ composites [J]. *Materials Transactions*, 2001, 42(6): 1007–1014.
- [8] STOBRAWA J, CIURA L, RDZAWSKI Z. Rapidly solidified strips of Cu–Cr alloys [J]. *Scrip Mater*, 1996, 34(11): 1759–1763.
- [9] BATRA I S, DEY G K. Microstructure and properties of a Cu–Cr–Zr alloy [J]. *Journal of Nuclear Materials*, 2001, 299(2): 91–100.
- [10] HOLZWARTH U, STAMM H. The precipitation behaviour of ITER-grade Cu–Cr–Zr alloy after simulating the thermal cycle of hot isostatic pressing [J]. *Journal of Nuclear Materials*, 2000, 279(1): 31–45.
- [11] HUANG F X, MA J S, NING H L, GENG Z T, LU C, GUO S M, YU X T, WANG T, LI H, LOU H F. Analysis of phases in a Cu–Cr–Zr alloy [J]. *Scrip Mater*, 2003, 48: 97–102.
- [12] XIA C D, JIA Y L, ZHANG W, ZHANG K, DONG Q Y, XU G Y, WANG M P. Study of deformation and aging behaviors of a hot rolled-quenched Cu–Cr–Zr–Mg–Si alloy during thermomechanical treatments [J]. *Materials and Design*, 2012, 39: 404–409.
- [13] XIE Hao-feng, MI Xu-jun, HUANG Guo-jie, GAO Bao-dong, YIN Xiang-qian, LI Yan-feng. Effect of thermomechanical treatment on microstructure and properties of Cu–Cr–Zr–Ag alloy [J]. *Rare Metals*, 2011, 30(6): 650–656. (in Chinese)
- [14] LIN G B, WANG Z D, ZHANG M K, ZHANG H, ZHAO M. Heat treatment method for making high strength and conductivity Cu–Cr–Zr alloy [J]. *Materials Science and Technology*, 2011, 27(5): 966–969.
- [15] BISELLI C, GUNTHER S, MORRIS M A, MORRIS D G. Thermo-mechanical processing of spray-formed Cu–Cr–Zr alloy [J]. *Scrip Metall Mater*, 1993, 29(6): 765–769.
- [16] APPELLO M, FENICI P. Solution heat treatment of a Cu–Cr–Zr alloy [J]. *Materials Science and Engineering A*, 1988, 102: 69–75.

CuZr/AlN 纳米复合材料的组织与性能

谷 曼^{1,2}, 吴玉程^{1,3}, 焦明华^{3,4}, 黄新民¹

1. 合肥工业大学 材料科学与工程学院, 合肥 230009;
2. 合肥学院 机械工程系, 合肥 230022;
3. 安徽省粉末冶金工程技术中心, 合肥 230009;
4. 合肥工业大学 摩擦学研究所, 合肥 230009

摘 要: 采用粉末冶金方法制备高强高导铜合金基纳米复合材料(CuZr/AlN)。采用光学显微镜(OM)和高分辨率透射电镜(HRTEM)等方法研究不同烧结工艺对复合材料组织与性能的影响, 研究固溶时效对 CuZr/AlN 力学性能的影响。结果表明: 试样的组织致密, 晶粒大小在 0.2 μm 左右; 试样的布氏硬度随着复压制压力和烧结温度的升高而升高; 试样的布氏硬度开始随着钨含量的增加而升高, 但当钨颗粒含量大于 0.5%时, 复合材料的布氏硬度开始降低。试样的抗弯强度随着复压制压力和烧结温度的升高而提高, 抗弯强度在钨含量为在 0.5%时最大。900 °C 固溶后的布氏硬度比固溶前的布氏硬度低, 试样在 500 °C 和 600 °C 时效后, 布氏硬度增加, 在 700 °C 发生过时效现象。

关键词: CuZr/AlN 纳米复合材料; 粉末冶金; 力学性能

(Edited by Hua YANG)